Regional gravity decrease after the 2010 Maule (Chile) earthquake indicates large-scale mass redistribution

Shin-Chan Han,[1,2] Jeanne Sauber,[1] and Scott Luthcke[1]

Received 13 September 2010; revised 21 October 2010; accepted 1 November 2010; published 9 December 2010.

[1] We report small but detectable changes in the GRACE satellites' relative trajectory after the M8.8 Maule, Chile earthquake on 27 February 2010 that can be used to delineate the shift in the gravity field. A gravity anomaly of −5 μGal with a spatial scale of 500 km was found east of the epicenter after the earthquake. Based on coseismic models, the long-wavelength negative gravity change is primarily the result of crustal dilatation as well as surface subsidence in the onland region. The offshore positive gravity anomaly predicted from finite fault coseismic models is considerably smaller because the gravity changes due to surface uplift and interior deformation are opposite in polarity. Our study suggests a role for large-scale gravity observations in deciphering changes of the Earth's interior during great earthquakes by filling in the seldom-observed long-wavelength spectrum of earthquake deformations as a complement to surface geodetic measurements and seismic data. **Citation:** Han, S.-C., J. Sauber, and S. Luthcke (2010), Regional gravity decrease after the 2010 Maule (Chile) earthquake indicates large-scale mass redistribution, *Geophys. Res. Lett.*, *37*, L23307, doi:10.1029/2010GL045449.

1. Introduction

[2] The earthquake on 27 February 2010 ruptured more than 600 km along strike (N18°E) and 60 km along dip (18°) in the area around Maule, Chile. It was the fifth largest earthquake during the last 100 years with the moment magnitude M_w of 8.8 and numerous aftershocks (more than 300 with magnitudes greater than 5.0) were reported in two months following the Maule event (U.S. Geological Survey, http://earthquake.usgs.gov/). In addition to (tele)seismic analysis [*Lay et al.*, 2010, and the references therein] and geodetic data acquisition and analysis, it was expected that the Gravity Recovery And Climate Experiment (GRACE) satellite data could measure coseismic change due to the large spatial scale and average slip of this great Chilean earthquake. For the Sumatra-Andaman earthquake (M_w 9.2), the gravity anomaly measured over an area greater than 1000 km in diameter around the epicenter was −15 μGal or larger in the Andaman Sea and about 10 μGal over the southwestern area of the Sunda trench. We interpreted the larger negative anomaly to be associated primarily with intrinsic density change (crustal dilatation) after the rupture [*Han et al.*, 2006]. Earlier studies found the GRACE data useful for testing alternate coseismic deformation mechanisms associated with the 2004 event [*Ogawa and Heki*, 2007; *Panet et al.*, 2007; *De Linage et al.*, 2009].

[3] By deploying two identical satellites and tracking the distance between them with the radar ranging instrument, the two satellites of the GRACE mission have been measuring changes in range-rate (i.e., relative speed between the two satellites separated by ~220 km) at the altitude of ~500 km in order to measure mass redistribution [*Tapley et al.*, 2005]. The range-rate between the satellites varies from positive to negative as the satellites move toward the positive mass anomaly and then away from it (see the auxiliary material).[1]

[4] In section 2, we report detectable changes in range-rate between two GRACE satellites before and after the earthquake. We analyzed those range-rate observations with coseismic finite fault models constructed primarily by teleseismic data in section 3. The spatial patterns of the regional gravity changes obtained by inversion of the range-rate data were presented in section 4 to quantify the spatial extent, location, and magnitude of the gravity changes due to the earthquake.

2. Satellite-to-Satellite Tracking Data

[5] In order to verify the existence of any detectable change in 'relative speed' (range-rate) along the satellite orbits after the earthquake, two weeks worth of GRACE range-rate (Level-1B) data [*Case et al.*, 2010] before and after the earthquake were compared. During this period, the GRACE satellites' ground tracks presented unintended repeat patterns changing with orbital altitudes. The co-located ground tracks allow us to examine the range-rate data more easily to find sudden changes only with time because the effects caused by difference in spatial locations are substantially reduced.

[6] Figure 1a shows the ground tracks of the GRACE satellites two weeks before and after 27 February 2010 with a background map showing the coseismic gravity change predicted from a reference teleseismic model (UCSB model by Shao et al., 2010, see the auxiliary material). We chose data spanning two weeks from the ascending (moving from south to north) tracks near the epicenter. After applying a low pass filter to reduce instrumental noise at higher frequencies, the range-rate data along the satellite orbits are shown in Figure 1b. The GRACE data before and after the rupture are depicted on the right and the predicted range-rate changes computed from a priori models of seasonal and secular mass variations along the same orbits are shown on the left. The predicted changes were computed based on 6 years of GRACE data from 2004 to 2009. As expected, the signals over the Amazon basin, Patagonia glacier, and Antarctica peninsular are responsible for large variations in the GRACE

[1]Planetary Geodynamics Laboratory, NASA Goddard Space Flight Center, Greenbelt, Maryland, USA.
[2]Also at GEST, University of Maryland Baltimore County, Baltimore, Maryland, USA.

Copyright 2010 by the American Geophysical Union.
0094-8276/10/2010GL045449

[1]Auxiliary materials are available in the HTML. doi:10.1029/2010GL045449.

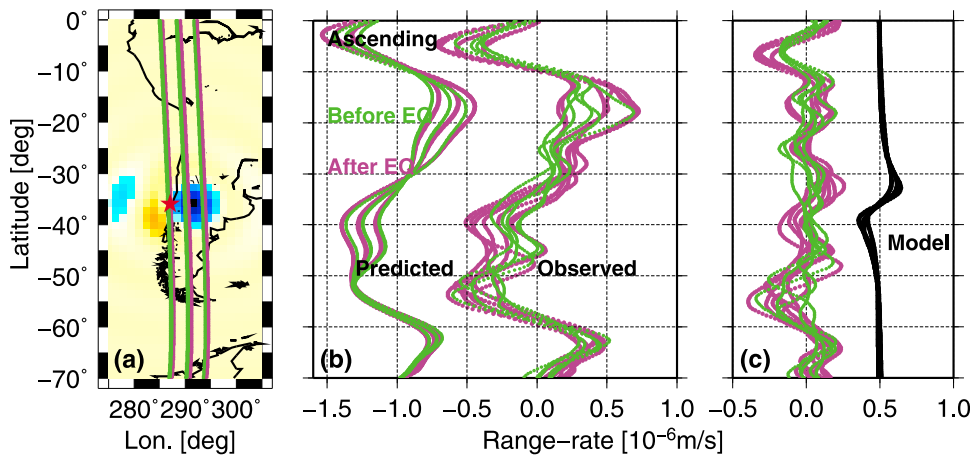

Figure 1. GRACE observations of range-rate change before and after the earthquake in Maule, Chile on February 27, 2010. (a) Ground tracks from the ascending orbits, two weeks before (green) and after (magenta) the earthquake, are depicted on the background map showing the predicted gravity changes from our reference coseismic model. The red star indicates the epicenter. (b) The measurements of range-rate between two satellites. The left pair shows the effect from the predicted seasonal change before and after the earthquake. The right pair shows the low-pass filtered GRACE observations with a precision of ~0.05×10^{-6} m/s. (c) The 'residual' observations after removing the predicted seasonal changes. The right curves show the predicted change computed from our reference coseismic model. The similar data from the descending orbit and offshore are available from the auxiliary material.

observations. The three distinct curves appeared in the predicted range-rate are due to slight transition in longitudes of the ground tracks. The range-rate changes expected by seasonal and secular mass variations two weeks before and after the earthquake (i.e., temporal changes) is smaller than the effects caused by different longitudes (i.e., spatial changes).

[7] The predicted changes were removed from observed range-rates and the residuals are shown in Figure 1c with the range-rate changes along the same orbits computed from the teleseismic model. A distinct feature varying from the negative to the positive values in range-rate as the satellites move from south to north is found from the model and the GRACE observations (only after the earthquake) with the peaks occurring at ~40°S and ~32°S. From the expected orbital motion of two satellites in response to the local mass anomaly discussed in the auxiliary material, one can infer the negative gravity anomaly after the earthquake. The observations present other signals as well, which are the residual mass variations in various regions. For example, over the Amazon, although the majority of seasonal changes were removed a priori, the residual temporal changes in Figure 1c are as large as the expected changes due to the earthquake found in the latitude band from 30°S to 40°S. The same sets of observations and models but along the descending tracks are shown in Figure S1. Just like the ascending track data, the negative-to-positive changes in range-rate along the orbits (from north to south for the descending track) are found in the data after the earthquake. The GRACE data over the ocean, where the predicted coseismic gravity change is small, are presented in Figures S2 and S3. The spatial and temporal changes in range-rate observations are considerably smaller than the data over the land. There is no significant change found from the ocean data before and after the rupture. It indicates that the gravity change associated with the earthquake will be largely over the land in accordance with what is predicted from the coseismic model. We will analyze what mechanism is responsible for this observation.

[8] We took the time-derivative of the GRACE range-rate data and compute the along-track range-acceleration to emphasize the regional anomaly caused by earthquake. We compared one month worth of the GRACE data before and after the earthquake in Figure 2. The data confined within the longitudes only from 285°E to 295°E were used since the earthquake signals in the satellite data decrease further away from the epicenter along longitude as well as latitude. The computed range-acceleration along the GRACE orbits from the seismic model was also depicted for the data after 27 February 2010. The positive range-acceleration anomalies localized within the latitude band from 40°S to 30°S are found from the data for the post-earthquake period. The positive range-acceleration anomaly indicates the relative speed (range-rate) change from the negative to the positive values as two satellites approach to and move away from the mass anomaly after the earthquake. The observations after the earthquake are consistent with the calculation from the coseismic finite fault model. More interestingly, the GRACE data distinguish the differences among seismic models as shown in the bottom two panels of Figure 2. More comprehensive GRACE data every two weeks from January to April in 2010 is shown in Figure S4.

3. Gravity Change Predicted From Finite Fault Models

[9] Various finite fault models of the 2010 Maule earthquake, representing the direction and amount of the slip on the pre-defined fault planes, were analyzed by computing their effects on the global gravitational field. The models are available from the references given in the auxiliary material. We used the analytic expression derived by *Pollitz* [1996, 1997] to compute the coseismic deformation and gravity anomaly from earthquake faults in a layered spherical Earth, based on the normal mode summation. For gravity anomaly, he considered the effects of radial deflection of density

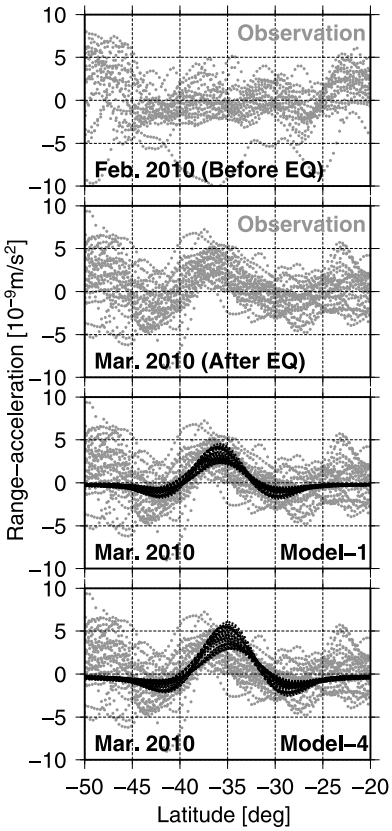

Figure 2. The low-pass filtered range-acceleration from GRACE (gray) with a precision of ~1×10^{-9} m/s^2. One month of the observations before (February) and after (March) the earthquake are shown. The computed range-accelerations, which accentuate the differences between the two coseismic models, are shown with the March data. Model-1 predicts the peak at 34°S while Model-4 does at 35°S due to the different locations of the major asperity.

stratification and compression and dilatation of the interior material following the ideas from *Okubo* [1992] who formulated the problem in a homogeneous half-space.

[10] The effects of surface and interior deformation on the gravitational potential were calculated separately and are shown in Figure 3. As noted by *Pollitz* [1997], the former is the gravitational attraction due to vertical deflection of the free surface. The latter is combination of intrinsic density change and a smaller contribution from the vertical displacement of internal density stratification. Figure 3a shows the power spectrum in terms of coseismic geoid change as a function of degree. The gravity spectra of the two effects are quite distinct. Over the low degrees, the gravitational effect of interior deformation exceeds the one of surface deformation. In contrast, over the degrees greater than 30, the surface deformation dominates the gravity contribution. The density contrast between ocean and crust was used to compute the gravity effect caused by the free surface radial displacement.

[11] Figure 3b presents the corresponding maps of the gravitational fields computed from the coseismic model, but truncated at degree and order 40. The surface deformation is characterized by a positive gravity anomaly offshore Maule due to uplift of the hanging wall. Across the region, however, the interior deformation is large with the extensional pattern perpendicular to the strike direction. Over the ocean, the two effects are similar in magnitude but opposite in sign and therefore any anomaly associated with the earthquake is small. Consequently, the negative gravity anomaly appears mostly on the land.

[12] The initial earthquake model presented in Figure 3 is based on teleseismic data (Model-1). In addition, we compared three other early coseismic slip models. The one from USGS (Model-2) is similar with Model-1 in magnitude and distribution of slip vectors, but including larger slip in a northern asperity. In contrast, the slip model Model-3 and the one from *Lay et al.* [2010] (Model-4) are smaller and greater than Model-1 and -2, respectively (Figure S5). The gravity effects of these four models were compared with the GRACE instantaneous range-acceleration measurement (Figure S6).

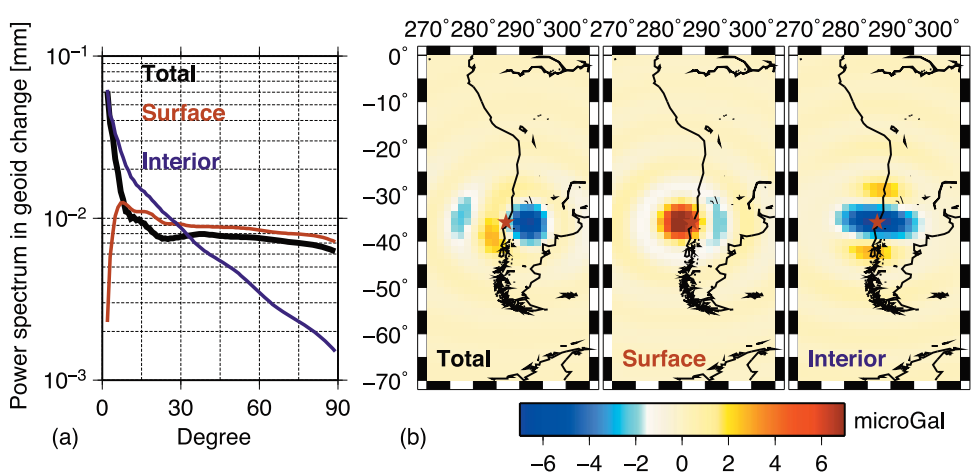

Figure 3. The predicted gravity change from a seismically-constrained finite fault model. (a) Power spectrum of the coseismic geoid change due to deformation at the surface (red) and in the interior (blue) and the total (black). (b) The respective spatial distribution of gravity changes. Note that the positive gravity anomaly associated with surface uplift is largest offshore whereas the negative anomaly due to interior change spans both the offshore and onshore regions.

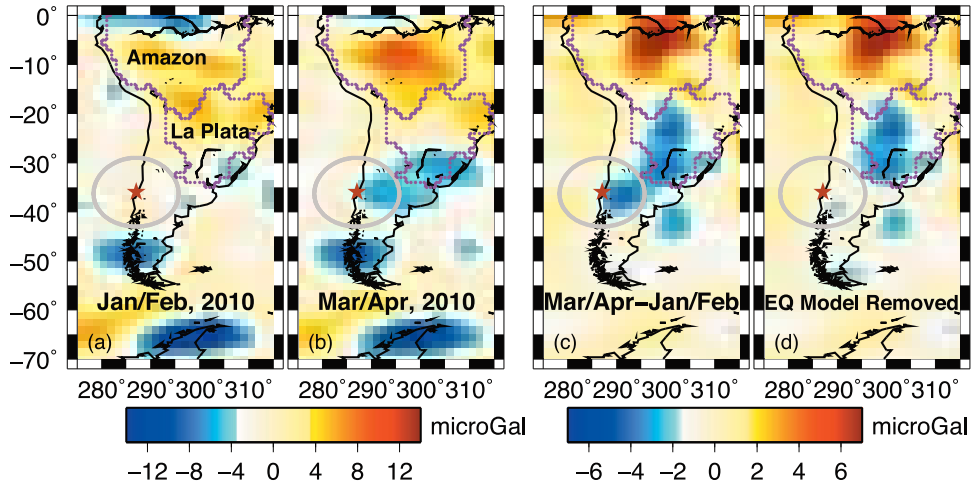

Figure 4. GRACE observations of regional gravity change with a precision of 2 μGal at the spatial resolution of 500 km. (a) The mean gravity anomaly estimated from two months worth of range-rate data from January to February in 2010 (excluding the last two days in Feb. assumed to be affected by the earthquake). (b) The same for Figure 4a but from two months data after the earthquake. Note that the soil moisture and snow mass was removed in Figures 4a and 4b based on a hydrology model. (c) The difference between Figure 4b and Figure 4a. (d) The residual gravity change with the earthquake effect removed on the basis of a finite fault model. Two major river basins (Amazon and La Plata) are delineated by dashed purple lines.

In general, the gravity response is proportional to the slip vectors given that the fault geometry parameters are the same. As also shown in Figure 2, the difference in location and magnitude of the major asperities particularly between the two models, Model-1 and -4, is testable with the range-rate data at a detectable level. However, care must be taken when the coseismic models and GRACE are compared, because the GRACE data includes the effect of early postseismic deformation.

4. Observed Gravity Change

[13] The spatial distribution of the gravity change was estimated by inversion of the GRACE range-rate data. A pair of mean time-variable gravity fields before and after the earthquake was estimated with two months worth of data for each and is shown in Figures 4a and 4b. The negative anomalies over the Patagonia and Antarctic peninsula, found consistently from both maps, are due to glacier ice mass loss [*Chen et al.*, 2007] with respect to the applied reference gravity field GGM02C [*Tapley et al.*, 2005] that represents the mean gravity field over the periods in 2002 and 2003. The anomalies over the Amazon and La Plata river basins show gradual changes from January through April in 2010, as expected from the seasonal changes in water storage. The soil moisture and snow mass components were partially reduced a priori on the basis of the GLDAS model [*Rodell et al.*, 2004] by removing such contributions to the GRACE range-rate data directly before the inversion.

[14] The difference between the two solutions, depicted in Figure 4c, shows an increasing trend in water storage around the central Amazon, which is mostly due to surface water storage not modeled in GLDAS. A decreasing trend around the La Plata basin is due to decreasing precipitation during the period under consideration. The negative anomaly was also found around the epicenter. It is not likely associated with hydrological water mass variation since there is no apparent river basin that can retain as much water as the Amazon or La Plata basins do. We applied the earthquake model (Model-1) in order to remove the predicted earthquake effect on range-rate from the data in March and April before the gravity inversion. Then, based on these new range-rate data (excluding the earthquake signal from Model-1), we made another inversion for the gravity field from March through April 2010. The difference between the new Mar/Apr solution and the previous Jan/Feb solution is shown in Figure 4d. The signal found around the epicenter disappeared, indicating such anomaly is most probably due to coseismic deformation. This forward modeling of earthquake signal to range-rate helps avoid aliasing error and leakage that often hinder the analysis of global GRACE gravity data.

5. Summary and Discussion

[15] The 2010 Maule earthquake disturbed the orbital motion of the GRACE satellites to a detectable level. The abrupt change in the gravity field by −5 μGal with a spatial scale of 500 km was found east of the epicenter but no significant gravity change was found offshore. The dimension and magnitude of the negative anomaly is similar to or less than seasonal variation of water mass within large South American river basins. Based on our gravity computation with coseismic finite fault models, we suggest that the crustal dilatation and surface subsidence is responsible for the negative gravity anomaly observed on the land, whereas the predicted positive gravity anomaly of surface uplift over the ocean (west of the Peru-Chile trench) was reduced by the ocean mass and by the negative anomaly of interior density change. Similar to the 2004 Sumatra-Andaman earthquake, the interior mass redistribution was found to be important at a large spatial scale. As a result of postseismic relaxation over the few months spanned by our GRACE observations, the actual coseismic gravity change might be larger than what we report in this study. As we learned from the 2004 Sumatra-

Andaman event [*Han et al.*, 2008], the temporal pattern of postseismic gravity change will help advance our understanding of the rheology and viscosity structure around the subduction zone between South America and Nazca plates.

[16] Finally, the comparison of various finite fault models with 'raw' GRACE range-rate data illustrates the possibility to constrain the fault slip vectors directly from the GRACE range-rate data. Teleseismic data have limitation on resolving dip angle and slip separately and GPS data are distributed only in the eastern areas on land that may cause biases in slip estimates. The GRACE range-rate data covering larger areas will be useful to verify and constrain the earthquake model parameters independently.

[17] **Acknowledgments.** This work was supported by NASA GRACE projects and Earth Surface and Interior program. We thank DLR for providing the GRACE telemetry data and JPL for producing the high-quality Level-1B products. David Rowlands is acknowledged for explanation on two GRACE satellites. We thank Chen Ji, Thorne Lay, Charles Ammon, and Anthony Sladen for coseismic finite fault models and Fred Pollitz for numerical codes to compute coseismic displacement and gravity change. The constructive comments from reviewers helped to improve the paper.

References

Case, K., G. Kruizinga, and S.-C. Wu (2010), GRACE level 1B data product user handbook, *JPL Publ.*, *D-22027*.

Chen, J., C. Wilson, B. Tapley, D. Blankenship, and E. Ivins (2007), Patagonia Icefield melting observed by Gravity Recovery and Climate Experiment (GRACE), *Geophys. Res. Lett.*, *34*, L22501, doi:10.1029/2007GL031871.

De Linage, C., et al. (2009), Separation of coseismic and postseismic gravity changes for the 2004 Sumatra–Andaman earthquake from 4.6 yr of GRACE observations and modelling of the coseismic change by normal-modes summation, *Geophys. J. Int.*, *176*, 695–714, doi:10.1111/j.1365-246X.2008.04025.x.

Han, S.-C., C. K. Shum, M. Bevis, C. Ji, and C. Kuo (2006), Crustal dilatation observed by GRACE After the 2004 Sumatra-Andaman earthquake, *Science*, *313*, 658–662, doi:10.1126/science.1128661.

Han, S.-C., J. Sauber, S. Luthcke, C. Ji, and F. Pollitz (2008), Implications of postseismic gravity change following the great 2004 Sumatra-Andaman earthquake from the regional harmonic analysis of GRACE intersatellite tracking data, *J. Geophys. Res.*, *113*, B11413, doi:10.1029/2008JB005705.

Lay, T., C. J. Ammon, H. Kanamori, K. D. Koper, O. Sufri, and A. R. Hutko (2010), Teleseismic inversion for rupture process of the 27 February 2010 Chile (Mw 8.8) earthquake, *Geophys. Res. Lett.*, *37*, L13301, doi:10.1029/2010GL043379.

Ogawa, R., and K. Heki (2007), Slow postseismic recovery of geoid depression formed by the 2004 Sumatra-Andaman Earthquake by mantle water diffusion, *Geophys. Res. Lett.*, *34*, L06313, doi:10.1029/2007GL029340.

Okubo, S. (1992), Gravity and potential changes due to shear and tensile faults in a half-space, *J. Geophys. Res.*, *97*, 7137–7144, doi:10.1029/92JB00178.

Panet, I., et al. (2007), Coseismic and post-seismic signatures of the Sumatra 2004 December and 2005 March earthquakes in GRACE satellite gravity, *Geophys. J. Int.*, *171*, 177–190, doi:10.1111/j.1365-246X.2007.03525.x.

Pollitz, F. (1996), Coseismic deformation from earthquake faulting on a layered spherical Earth, *Geophys. J. Int.*, *125*, 1–14, doi:10.1111/j.1365-246X.1996.tb06530.x.

Pollitz, F. (1997), Gravity anomaly from faulting on a layered spherical Earth with application to central Japan, *Phys. Earth Planet. Inter.*, *99*, 259–271, doi:10.1016/S0031-9201(96)03204-9.

Rodell, M., et al. (2004), The Global Land Data Assimilation System, *Bull. Am. Meteorol. Soc.*, *85*, 381–394, doi:10.1175/BAMS-85-3-381.

Tapley, B., et al. (2005), GGM02—An improved Earth gravity field model from GRACE, *J. Geod.*, *79*, 467–478, doi:10.1007/s00190-005-0480-z.

S.-C. Han, S. Luthcke, and J. Sauber, Planetary Geodynamics Laboratory, NASA Goddard Space Flight Center, Code 698, Greenbelt, MD 20771, USA. (shin-chan.han@nasa.gov)